

This discussion paper is/has been under review for the journal Atmospheric Chemistry and Physics (ACP). Please refer to the corresponding final paper in ACP if available.

# Reconciliation of measurements of hygroscopic growth and critical supersaturation of aerosol particles in Southwest Germany

M. Irwin<sup>1</sup>, N. Good<sup>1</sup>, J. Crosier<sup>1,2</sup>, T. W. Choularton<sup>1</sup>, and G. McFiggans<sup>1</sup>

<sup>1</sup>School of Earth, Atmospheric and Environmental Sciences, University of Manchester, Manchester, UK

<sup>2</sup>National Centre for Atmospheric Science, University of Manchester, Manchester, UK

Received: 31 May 2010 – Accepted: 23 June 2010 – Published: 12 July 2010

Correspondence to: G. McFiggans (gordon.mcfiggans@manchester.ac.uk)

Published by Copernicus Publications on behalf of the European Geosciences Union.

## Reconciliation of hygroscopicity measurements during UK-COPS

M. Irwin et al.

Title Page

Abstract

Introduction

Conclusions

References

Tables

Figures

⏪

⏩

◀

▶

Back

Close

Full Screen / Esc

Printer-friendly Version

Interactive Discussion

## Abstract

Aerosol physical, chemical and hygroscopic properties were measured in a range of airmasses during COPS (Convective and Orographically-induced Precipitation Study) ground-based in June and July of 2007 at the Hornisgrinde mountain site in the Black Forest, Southwest Germany. Hygroscopic growth factors at 86% relative humidity were measured and critical supersaturation simultaneously derived for particles of dry diameters 27 to 217 nm, both properties exhibiting substantial variability with time and with particle size.

Variability in the measurements of hygroscopic growth factor and critical supersaturation for particles of similar sizes indicates significant compositional impact on particle water affinity. Critical supersaturation prediction using a single parameter hygroscopicity approximation derived from measured HTDMA mean growth factors deviate, beyond measurement uncertainties, from critical supersaturations derived from CCN measurements. These led to differences averaging around 35% in potential cloud droplet number concentration (CDNC) for the most reliable measurements depending on averaging methodology, often very much larger for individual time periods. This indicates aspects of water uptake behaviour unresolved in this experiment by the single parameter representation which, depending on its origin, may have important consequences on its generalised use.

## 1 Introduction

Atmospheric aerosol plays a key role in a number of important climate processes, commonly classified into direct effects (scattering and absorbing radiation; McCormick and Ludwig, 1967; Haywood and Boucher, 2000) and indirect effects (radiative effects that result from modifying the reflectivity, abundance, persistence and other cloud properties). The Intergovernmental Panel on Climate Change (IPCC) Fourth Assessment Report has attributed the largest uncertainty in radiative forcing to that of the aerosol

ACPD

10, 17073–17111, 2010

## Reconciliation of hygroscopicity measurements during UK-COPS

M. Irwin et al.

Title Page

Abstract

Introduction

Conclusions

References

Tables

Figures

⏪

⏩

◀

▶

Back

Close

Full Screen / Esc

Printer-friendly Version

Interactive Discussion



## Reconciliation of hygroscopicity measurements during UK-COPS

M. Irwin et al.

Title Page

Abstract

Introduction

Conclusions

References

Tables

Figures

⏪

⏩

◀

▶

Back

Close

Full Screen / Esc

Printer-friendly Version

Interactive Discussion



indirect effect (Forster et al., 2007). The first indirect effect, the cloud albedo effect, occurs because differences in cloud droplet number concentration (CDNC) alter the reflectivity of clouds (Twomey, 1977). Aerosol particles also have effects on cloud longevity and the initiation or delay of precipitation through increased CDNC, which are some of the secondary indirect effects on climate (Albrecht, 1989; Lohmann and Feichter, 2005; Andreae and Rosenfeld, 2008). Uncertainty in cloud condensation nuclei concentration (CCNC), whilst not directly reflected in CDNC owing to the competition between growing droplets for available water vapour, is central to the uncertainty in the aerosol indirect effects.

The ability for a particle to act as a CCN depends on its size and composition. Particles of a dry diameter less than 40 nm are unlikely to activate into cloud droplets regardless of composition and sufficiently large particles will most probably contain enough soluble material to activate under all reasonable atmospheric supersaturations (McFiggans et al., 2006). If a particle's composition is known, then its water uptake at equilibrium can be modelled using the Köhler equation (Köhler, 1936; Rogers and Yau, 1989; Pruppacher and Klett, 1997; Seinfeld and Pandis, 1998) based on physicochemical properties of the solute:

$$S = a_w \exp K_e \quad (1)$$

Where  $S$  is the saturation ratio ( $=RH/100$ ),  $a_w$  is the water activity or Raoult term, and  $K_e$  is the Kelvin term.

The Köhler equation can be envisaged as the competition between the Raoult effect, defined by the water activity and drawing water into the growing droplet by virtue of the soluble material therein and the Kelvin effect, defining the resistance to growth resulting from the increased saturation vapour pressure of water with increasing curvature of smaller particles by virtue of the energy associated with the creation of the droplet surface. The Köhler equation is dominated by the water activity when significantly below saturation and the Kelvin term increases in importance approaching the point of activation. The relative importance of the terms in the Köhler equation is explored systematically in Wex et al. (2008).

**Reconciliation of  
hygroscopicity  
measurements  
during UK-COPS**

M. Irwin et al.

Title Page

Abstract

Introduction

Conclusions

References

Tables

Figures

⏪

⏩

◀

▶

Back

Close

Full Screen / Esc

Printer-friendly Version

Interactive Discussion

The atmospheric aerosol is comprised of substantial amounts of organic material (Kanakidou et al., 2004; Hallquist et al., 2009), which may suppress surface tension (Facchini et al., 2000; McFiggans et al., 2005, 2006; Weingartner et al., 2008). Since the surface tension enters into the Köhler equation through the Kelvin term and it is known that organic components may reduce the surface tension of their aqueous solutions, it has been assumed that they may play a role in determining cloud activation (Abdul-Razzak and Ghan, 2004). If it were to occur, a change in surface tension would play a more important role as the saturation ratio increases (Wex et al., 2008), thus it has been argued that the incorporation of organic material into existing inorganic particles may substantially reduce the supersaturation required to activate an aerosol particle into a cloud droplet (its critical supersaturation,  $S_c$ ). Such an effect would result in an increase in the number of CCN by impacting on the Kelvin term, whilst not significantly influencing sub-saturated growth factor through impacts on the number of soluble molecules, affecting the Raoult term. However, bulk to surface partitioning has recently been postulated as occurring within a more detailed description of the surface chemistry which can increase the critical supersaturation required for activation by changing concentration gradients approaching the surface (Sorjamaa et al., 2004, 2006; Topping et al., 2007) acting to offset the reduction in  $S_c$  predicted to result from reduced surface tension.

A current challenge is to demonstrate the quantitative understanding of atmospheric aerosol behaviour under sub- and supersaturated conditions and the relationship between the two regimes. Multiple field studies from around the world utilising a variety of modelling techniques have compared sub- and supersaturated measurements and model predictions (e.g., Broekhuizen et al., 2006 and references to CCN closure studies in McFiggans et al., 2006 and e.g., Medina et al., 2007; Petters and Kreidenweis, 2007, and references therein) with varying degrees of success. The latter reference presented the  $\kappa$ -Köhler model, making use of a single parameter  $\kappa$  to describe particle hygroscopicity at any humidity. This approach can demonstrably reconcile sub- and supersaturated behaviour of inorganic salts such as sodium chloride within experimental

uncertainty, and the use of  $\kappa$  to describe the hygroscopicity of ambient aerosol populations has been explored previously (Andreae and Rosenfeld, 2008; Gunthe et al., 2009).

In this study we use the  $\kappa$ -Köhler model to interpret data from both sub- and super-saturated regimes measured at a continental forest site with strong topographical and convective influences on cloud formation, aiming to reconcile particle water uptake in the two regimes.

## 2 Experimental methodology

### 2.1 Sampling site and measurement platform

Measurements were conducted from 24 June to 18 July 2008 as part of the Convective and Orographically forced Precipitation Study (COPS) at the Hornisgrinde SuperSite (48°36′0″ N, 8°12′0″ E), which is located in the Western Black Forest in Germany. The Hornisgrinde Mountain is at a height of 1164 m a.s.l. and the moorland area at the summit of the Hornisgrinde is a nature reserve with pedestrian access and little vehicle activity. Further details of the measurement site and the COPS programme are presented in detail by Wulfmeyer et al. (2008).

Air was drawn down a 40 mm bore, 3 m high stainless steel stack at a flow rate of 35 l/min, through a cyclone impactor with a 4  $\mu$ m cut-off, and then into the container to the instrumentation which, excepting the water uptake measurement instrumentation outlined in Sects. 2.2 and 2.3, is described in more detail in Jones et al. (2010).

### 2.2 Sub-saturated water uptake measurement

A Hygroscopicity Tandem Differential Mobility Analyser (HTDMA; Cubison et al., 2005; Gysel et al., 2007) was used to measure the hygroscopic growth factor distributions at 86% relative humidity (RH) of particles with dry diameters ( $D_0$ ); 27, 43, 85, 127,

## Reconciliation of hygroscopicity measurements during UK-COPS

M. Irwin et al.

Title Page

Abstract

Introduction

Conclusions

References

Tables

Figures

⏪

⏩

◀

▶

Back

Close

Full Screen / Esc

Printer-friendly Version

Interactive Discussion



169, 211 and 254 nm. The hygroscopic growth factor of a particle is defined as  $GF_{D_0, 86\%} = D_{86\%} / D_0$  where  $D_{86\%}$  is the diameter at 86% RH. To ensure the HTDMA instrument was measuring reliably, the instrument was calibrated as described in Good et al. (2010). Briefly, the laminar flow elements and pressure transducers controlling flow through the Differential Mobility Analysers (DMAs) were calibrated using a bubble flowmeter and the DMAs were size-calibrated using NIST-traceable polystyrene latex spheres (PSLs). The RH and temperature sensors within the instrument (Cubison et al., 2005) were calibrated and continuously referenced against a dew point hydrometer. Dry (RH  $\leq$  15%) scans were performed at weekly intervals to ensure that both the DMAs were in agreement, to monitor the width of the DMA transfer functions, to measure the offset between the two DMAs as well as any temporal trend (Gysel et al., 2009; Good et al., 2010). The HTDMA system was calibrated with dried, charge-neutralised 150 nm ammonium sulphate and sodium chloride ( $\geq$  99.5%, Sigma Aldrich) such that the RH of the second DMA was increased slightly beyond the measurement range (to typically greater than 90% RH). Both deliquescence and effloresced points for both salts are measured by the HTDMA and verified against the ADDEM model (Topping et al., 2005).

The first DMA was used to select dry particle size with dry sheath air and a residence time of  $\sim$ 60 s was included between the humidifier and the second DMA (Cubison et al., 2005; Gysel et al., 2007). The second DMA was operated with both sheath and aerosol flows at a target RH of 86%, as due to unforeseen circumstances the instrument struggled to reach 90% RH whilst sampling ambient aerosol, and the decision was made to sample at a lower RH with greater stability. The target of 86% RH was reached for the majority of the experiment with variability between 84–88% RH. The second DMA voltage (and thus mobility diameter) was stepped through each  $D_0$  to measure the raw particle diameter growth factor distribution. These raw data were inverted to account for the HTDMA instrument function using the TDMA<sub>inv</sub> algorithm along with the associated analysis and quality assurance procedures described by Gysel et al. (2009).

Further to inversion, data measured between 84%–88% RH were corrected to 86%

## Reconciliation of hygroscopicity measurements during UK-COPS

M. Irwin et al.

Title Page

Abstract

Introduction

Conclusions

References

Tables

Figures



Back

Close

Full Screen / Esc

Printer-friendly Version

Interactive Discussion

RH, and an error simulation showing the sensitivity of the inversion result to small changes in measurement was performed as described by Gysel et al. (2009). The results of the error simulation and the propagation of measurement uncertainty as standard errors are described in detail by Irwin et al. (2010). From the analysis and error propagation, the mean of the particle growth factor probability distribution becomes the corrected mean growth factor,  $GF_{D_0, RH, \text{mean}, \text{corr}}$ .

### 2.3 Droplet activation measurement

A Droplet Measurement Technologies (DMT) Cloud Condensation Nucleus counter (CCNc; Roberts and Nenes, 2005) was used to probe the activation behaviour of the sampled particles. The CCNc instrumental configuration was alternated between sampling poly-disperse and mono-disperse aerosol. To generate a monodisperse aerosol, polydisperse aerosol was charge equilibrated then size selected in a DMA. This monodisperse aerosol was then split between the CCNc and a 3010 TSI Condensation Particle Counter (CPC) with the sample line lengths from the DMA to the CPC inlet and top of the CCNc column matched in order to ensure line losses were equal. For each mobility-selected size, the ratio of CCN to CPC concentration defines the activated fraction at a given supersaturation. The dry diameter range for monodisperse CCNc measurement was in the range 25–250 nm. Particles just below their critical supersaturation may have a large unactivated equilibrium size that can be of the same order as activated droplets ( $\approx 1 \mu\text{m}$ , Lance et al., 2006) and particles were judged to have activated when detected by the OPC in the CCNc at diameters above  $1 \mu\text{m}$ .

Perfectly monodisperse internally mixed particles would all activate at a single discrete supersaturation such that 100% of the particles would be unactivated at an infinitesimally lower supersaturation, but activated at an infinitesimally higher value. In reality, the monodisperse selection will be of finite dispersion with broadening defined by the DMA transfer function. In addition, as found by Rose et al. (2008) there is an indeterminate contribution to the “system transfer function” such that deviation in the observed CCN spectrum from a step change in the activated fraction does not result

## Reconciliation of hygroscopicity measurements during UK-COPS

M. Irwin et al.

Title Page

Abstract

Introduction

Conclusions

References

Tables

Figures

⏪

⏩

◀

▶

Back

Close

Full Screen / Esc

Printer-friendly Version

Interactive Discussion



## Reconciliation of hygroscopicity measurements during UK-COPS

M. Irwin et al.

Title Page

Abstract

Introduction

Conclusions

References

Tables

Figures

⏪

⏩

◀

▶

Back

Close

Full Screen / Esc

Printer-friendly Version

Interactive Discussion

from the ideal transfer function of the DMA alone. Assuming that the transfer function is symmetrical about the selected dry mobility, the supersaturation at which 50% of the particles have activated into cloud droplets was directly interpreted as representing  $S_{c,D_0}$ . Variations in the hygroscopicity of particles of the same  $D_0$  may lead to further spectral broadening, affecting the interpretation of  $S_{c,D_0}$ . The impacts of such deviations from a perfectly internally-mixed particle population is discussed later. In addition to deriving  $S_{c,D_0}$ , the diameter at which 50% of the particles activated into cloud droplets was derived at each supersaturation;  $D_{50,S}$ .

The benefit of the  $S_{c,D_0}$  analysis is that the critical supersaturation for multiple dry diameters can be measured on an hourly basis. The  $D_{50,S}$  analysis however typically has a smaller associated fitting error resulting from the increase in the number of data points used in each sigmoidal fit ( $\sim 20 D_0$  for each of the five supersaturations). The derivation of hygroscopicity parameter  $\kappa$  from  $S_{c,D_0}$  is described in Sect. 2.5 and an explanation of how measurement uncertainty is propagated through this derivation as standard errors is described by Irwin et al. (2010). The number of CCN that may potentially be activated as cloud droplets at any given size can be obtained from measured size distributions and either  $\kappa_{S_{c,D_0}}$  or  $S_{c,D_0}$  as described in Sect. 3.6.

CCN instrument calibration involved the sampling of nebulised, dried, charge-equilibrated, and size-selected ammonium sulphate ( $\geq 99.5\%$ , Sigma Aldrich) and sodium chloride ( $\geq 99.5\%$ , Sigma Aldrich) aerosol particles with a TSI 3010 CPC and the CCNc. The measured  $S_c$  was plotted against the predicted  $S_c$  of ammonium sulphate particles of the same dry diameter as calculated using the ionic interaction model within the Aerosol Diameter Dependent Equilibrium Model (ADDEM; Topping et al., 2005). A  $\Delta T$  dependent calibration factor was applied such that the calibrated supersaturation setpoints were 0.11%, 0.17%, 0.32%, 0.50% and 0.80% (the supersaturation range was increased from 0.11%, 0.17%, 0.28%, 0.35% and 0.65% after the first week, 25 June–3 July, after reviewing the aerosol activation behaviour).

The effects of multiple charging were found to be negligible due to the shape of the aerosol number-size distribution. Nevertheless, the dataset was corrected for the

## Reconciliation of hygroscopicity measurements during UK-COPS

M. Irwin et al.

Title Page

Abstract

Introduction

Conclusions

References

Tables

Figures

⏪

⏩

◀

▶

Back

Close

Full Screen / Esc

Printer-friendly Version

Interactive Discussion



effects of multiply charged particles in standard DMPS procedure, using the charging probability coefficients found by Wiedensohler (1987) as reported in Good et al. (2010). As the container was air conditioned to  $20^{\circ}\text{C}\pm 2^{\circ}\text{C}$ , the set point supersaturations corresponded to a near-constant  $\Delta T$  and thus absolute  $T$ , ensuring validity of the calibration. In addition to calibrations, uncertainty in the measurements have been propagated through the data analysis as described in Irwin et al. (2010). Hourly switching of the DMA-CCNc instrumentation between polydisperse and monodisperse operation continued throughout the project. When the CCNc was running in polydisperse mode, the CPC was used in the Differential Mobility Particle Sizer (DMPS; Williams et al., 2007) instrument. During monodisperse operation, the DMA supplied the CCNc and CPC as outlined above. Only results from this latter mode of operation are presented here.

A more complete description of the calibration, quality assurance procedures and error propagation carried out for the two instruments is presented by Good et al. (2010) and Irwin et al. (2010).

### 2.4 Aerosol composition

A High-Resolution Time-of-Flight Aerosol Mass Spectrometer (HR-ToF-AMS, Aerodyne Research Inc.) was used to probe non-refractory aerosol particle composition (DeCarlo et al., 2006). The instrument was operated with a heater temperature of approximately  $550^{\circ}\text{C}$  and is capable of measuring particles from 40 nm–700 nm vacuum aerodynamic diameter (Decarlo et al., 2004). The mass size distribution of the aerosol particles was measured in particle mode. The collection efficiency used for the COPS data was 0.5, which is consistent with results from laboratory (Matthew et al., 2008) resulting in broad agreement with the integrated submicron volume time series from the DMPS.

## 2.5 Predicting $S_c$ from measured HTDMA $GF_{D_0}$

The  $\kappa$ -Köhler model represents water activity ( $a_w$ ) in terms of a constant ( $\kappa$ ) within the primitive Köhler equation (Eq. 1) assuming a constant value for surface tension within the Kelvin term:

$$S = \frac{D^3 - D_0^3}{D^3 - D_0^3(1 - \kappa)} \exp\left(\frac{4\sigma_w M_w}{RT \rho_w D}\right) \quad (2)$$

Where  $D$  is the droplet diameter at the given RH,  $D_0$  is dry particle diameter,  $\sigma_w$  is the surface tension of water,  $M_w$  is the molecular weight of water,  $R$  is the universal gas constant,  $T$  is the droplet temperature and  $\rho_w$  is the density of water.

To examine the applicability of the  $\kappa$ -Köhler approach taken by Petters and Kreidenweis (2007),  $\kappa$  is derived from measured HTDMA-determined values of the hygroscopic diameter growth factor. Substituting  $GF_{D,RH}$  into Eq. (2), the  $\kappa$ -Köhler equation for a defined RH becomes:

$$RH = \frac{GF_{D_0,RH}^3 - 1}{GF_{D_0,RH}^3 - (1 - \kappa)} \exp\left(\frac{4\sigma_w M_w}{RT \rho_w D_0 GF_{D_0,RH}}\right) \quad (3)$$

$S_{c(\kappa, GF_{D_0,RH,mean,corr})}$  is predicted for a given droplet diameter using Eq. (3) with  $\kappa_{(GF_{D_0})}$  and incrementally increasing the growth factor until the relative humidity starts to decrease. As with traditional Köhler theory, the maximum in  $S$  for a given size and composition (expressed by  $\kappa$ ) determines  $S_c$  for activation to a cloud droplet (Petters et al., 2007).

## 2.6 Error analysis

In order to investigate whether the sub- and supersaturated water uptake behaviour can be reconciled within the measurement uncertainty, it is necessary to propagate the errors associated with each step in the analysis into each level of data product. A full

### Reconciliation of hygroscopicity measurements during UK-COPS

M. Irwin et al.

Title Page

Abstract

Introduction

Conclusions

References

Tables

Figures

⏪

⏩

◀

▶

Back

Close

Full Screen / Esc

Printer-friendly Version

Interactive Discussion



description of the uncertainty analysis and error propagation is presented by Irwin et al. (2010).

Briefly, the measurements of both the HTDMA and CCNc have been broken down into primary and secondary data quantities, with the measurement uncertainty at each stage quantified as standard error. These standard errors can be propagated through to higher order data products in order to better interpret the results of any comparison or the conclusions drawn.

### 3 Results and analysis

#### 3.1 Meteorological conditions

For the majority of the experiment, the wind originated from West of Southwest, flowing up the valley (see Fig. S1 in supplementary material). Throughout the experiment the measurement site was frequently within cloud, with ambient RH sensors saturating at 100% (Fig. S2 in supplementary material). Out-of-cloud conditions often resulted from cloud base rising well above the measurement platform. The beginning of the measurement period (24 June–28 June) was characterised by cloud cover and some rainfall. The period of 29 June–2 July was mostly clear, with a distinct cloud event on the 30 June. The site was in cloud from 2–6 July, and again from 9–14 July. The final days of the measurement were characterised by clear, sunny days and low RH. Cloudy and out-of-cloud sampling periods were distinguished according to aerosol number concentrations as measured by a GRIMM Optical Particle Counter ( $0.3\ \mu\text{m} \leq D \leq 20\ \mu\text{m}$  in conjunction with ambient RH data (GRIMM concentration  $\leq 100$  and  $\text{RH} \geq 95\%$ ). These periods have been broadly approximated for contiguous representation and are described in Table 1.

During cloud periods, accumulation mode particle concentrations were low, as the activated aerosol formed droplets larger than the inlet cyclone cut of  $4\ \mu\text{m}$ . There were periods when high concentrations of particles ( $> 1000\ \text{cm}^{-3}$ ) of  $D_0 \leq 20\ \text{nm}$  were

## Reconciliation of hygroscopicity measurements during UK-COPS

M. Irwin et al.

Title Page

Abstract

Introduction

Conclusions

References

Tables

Figures

⏪

⏩

◀

▶

Back

Close

Full Screen / Esc

Printer-friendly Version

Interactive Discussion



observed in both cloudy and out-of-cloud periods. Each out-of-cloud period was characterised by high concentrations of particles with  $D_0 \geq 30$  nm a matter of hours after the RH dropped to below 80%, with the distribution exhibiting apparent growth over the course of the day to an average  $D_0$  of 100 nm (Fig. S2 in supplementary material). It is apparent that there was a significant dynamical evolution of the observed aerosol throughout the experiment.

### 3.2 Aerosol composition

The organic:sulphate mass ratio, as diagnosed from the HR-ToF-AMS, averaged 3:1 over the course of the project, with significant variability (see Fig. S2 in supplementary material). The organic:sulphate ratio tracks the organic:inorganic ratio well, with the majority of the variation in the organic:inorganic ratio coming from the variation in the sulphate component. Cloud periods are characterised by low accumulation mode number concentrations and lower mean organic:sulphate ratio (largely driven by enhanced sulphate loading), primarily seen in the second and fifth cloud periods, CP2 and CP5. A significant deviation from the mean was observed during the third out-of-cloud period, NC3, during which the organic:sulphate ratio was highly variable with peak ratio in excess of 8:1 and minima around 1:1. This highly variable period was followed by a more quiescent period and a reduction to the campaign mean ratio of 3:1 from the 17 July onwards. It should be noted that the meteorological influences on the aerosol composition were complex. All things being equal, one might expect sulphate aerosol to be preferentially scavenged by cloud and hence the organic to sulphate ratio to be enhanced in interstitial aerosol particles sampled under cloudy conditions. This was not clearly observed during COPS and the organic to sulphate ratio was frequently enhanced during no-cloud conditions. This was particularly noticeable during NC3. Prior to NC3, the cloud had been clearly advective and large-scale, with the possibility of large-scale in-cloud sulphate production leading to comparatively low organic:sulphate ratio. In contrast, the temperature (shown in the top panel of Fig. S2 in supplementary material) from this period onwards was warmer than before and the clear-sky condi-

## Reconciliation of hygroscopicity measurements during UK-COPS

M. Irwin et al.

Title Page

Abstract

Introduction

Conclusions

References

Tables

Figures



Back

Close

Full Screen / Esc

Printer-friendly Version

Interactive Discussion



tions were conducive to biogenic organic aerosol formation that may have led to the increased organic:sulphate ratio (Jones et al., 2010).

### 3.3 Hygroscopic behaviour in the sub-saturated regime

Growth factor probability densities were measured as described in Sect. 2.2 and are shown in Fig. 1 with a time resolution of 1h. For the majority of the measurement period a strong influence of particle size on hygroscopic growth is observed with the mean hygroscopic growth factor ( $GF_{D_0, RH, mean, corr}$ ) increasing from an average of 1.15 at 26 nm to 1.35 at 211 nm. For the majority of the experiment, the mean growth factor represents well the modal growth factor for each measured size, though at times there is increased bimodality at dry sizes greater than 127 nm. At all sizes, there is a fraction of the particles with low hygroscopicity (growth factor of  $\sim 1.15$ , similar to the mean seen at the lowest dry size,  $D_0=26$  nm) though with considerably reduced relative contribution at larger sizes. When the concentrations of the less hygroscopic mode are higher (NC1, NC2, CP3) the mean growth factor is reduced by up to 0.05 from the peak growth factor ( $GF_{D_0, RH, peak, corr}$ ), invariably found in the main, more hygroscopic mode.

The aerosol sampled during cloudy periods were, somewhat counter-intuitively, characterised by a low organic:sulphate ratio (as mentioned in Sect. 3.2 above), and this increase in relative sulphate is consistent with the slightly higher mean growth factors during these periods. Out of cloud mean growth factors tend to be lower in comparison, consistent with the increased mass fraction of organics, with a typical organic:sulphate ratio of  $\geq 4:1$ .

### 3.4 Measurements of cloud activation behaviour

The fraction of the particles at a given supersaturation ( $S$ ) and dry size ( $D_0$ ) that have activated into cloud droplets is defined as  $F_A = \frac{N_{S, D_0}}{N_{D_0}}$ .  $F_A$  typically increases with both dry size and supersaturation as shown in Fig. 2. Towards the latter part of the first half of the experiment, it was noted that the supersaturation settings  $S_{set}$  of 0.65% was not

## Reconciliation of hygroscopicity measurements during UK-COPS

M. Irwin et al.

Title Page

Abstract

Introduction

Conclusions

References

Tables

Figures

⏪

⏩

◀

▶

Back

Close

Full Screen / Esc

Printer-friendly Version

Interactive Discussion



activating all of the aerosol size distribution. The measurement range was increased to a ceiling of  $S_{\text{set}}=0.80\%$  as to improve the derivation of  $S_{c,D_0}$  for  $D_0$  below 100 nm. At the lowest supersaturation (0.11%) only sizes with  $D_0$  over 200 nm activate for the majority of the measurement period. As is expected,  $F_A$  increases with increasing supersaturation, until at the highest supersaturation (0.80%) almost all particles activate. For the majority of the experiment, each supersaturation could be characterised with a “threshold diameter” above which all particles activate.

Though variations throughout the experiment are evident in the activated fraction at each supersaturation (Fig. 2), these do not systematically vary with changes in the ratio of organic to sulphate mass loading (Fig. S2 in supplementary material). However CP2, NC2 and CP3 show some variability in  $F_A$ , but these periods are also characterised by low temporal resolution due to low number concentrations between  $50\text{ nm} < D_0 < 200\text{ nm}$ . CP3 is characterised by an increase in  $F_A$  across the size distribution, which may be expected as the threshold diameter for activation at a given supersaturation would increase when sampling from within a cloud, as the instrument would then be sampling interstitial particles which have not activated into cloud droplets. In addition, the organic:sulphate ratio (Fig. S2 in supplementary material) is somewhat higher for CP3 than for other cloud periods. The large difference between NC3 and CP4 in terms of the organic:sulphate ratio (10:1 down to 1:1, Fig. S2 in supplementary material) is not reflected in the activation ability of the aerosol across the size distribution. This is considered further in Sect. 3.6. It should be noted that size resolved measurements were unavailable at high time resolution and hence any systematic difference may be masked by time or size averaging of the composition.

Figure 3 shows a contour plot of  $S_{c,D_0}$  calculated for the entire project as described in Sect. 2.3. The supersaturation range 0.11%–0.65% was increased as previously described to 0.11%–0.80%. This increased data range typically reduced fitting errors and allowed for the derivation of  $S_{c,D_0}$  for smaller particle sizes; illustrated by the inclusion of  $S_{c,D_0}$  for  $50\text{ nm} < D_0$  (Fig. 3). Whilst some variation in  $S_{c,D_0}$  is evident between in and out-of-cloud periods and consistent with the variation in activated fraction, no

## Reconciliation of hygroscopicity measurements during UK-COPS

M. Irwin et al.

Title Page

Abstract

Introduction

Conclusions

References

Tables

Figures

⏪

⏩

◀

▶

Back

Close

Full Screen / Esc

Printer-friendly Version

Interactive Discussion

systematic difference was found between high and low organic to sulphate periods and  $S_{c,D_0}$ .

Whilst size resolved measurements were unavailable at high time resolution AMS compositional data was converted from vacuum aerodynamic diameter to mobility diameter using the methods described in Decarlo et al. (2004) and assuming a typical density for aged organics of  $1400 \text{ kg m}^{-3}$  (Sjogren et al., 2008) and averaged over the periods of high and low organic to sulphate ratios. Particles over 100 nm have an increased organic to sulphate content with a peak at around 300 nm which was above the measurement range for both the HTDMA and CCNc during this experiment (see Fig. S3 in supplementary material).

### 3.5 Reconciliation of the hygroscopicity and droplet activation measurements

The methodology used for the reconciliation and the propagation of errors in measurement are explained in detail by Irwin et al. (2010). The following section will aim to describe briefly and summarise the processes involved in this reconciliation.

For each dry size measured, values of  $\kappa$  were calculated by inserting  $GF_{D_0,RH,mean,corr}$  data into Eq. (2). The derived  $\kappa$  value and  $GF_{D_0,RH,mean,corr}$  were held constant whilst the RH was increased until reaching a maximum, thereby obtaining  $S_{c(\kappa,GF_{D_0,RH,mean,corr})}$  for each dry size.  $\kappa$  values were evaluated at a constant assumed surface tension equal to that of pure water ( $72.5 \text{ mNm}^{-1}$  at 298 K) and also at a range of suppressed  $\sigma$  values.

$S_{c,D_0}$  was calculated from CCNc data, where possible, in the same fashion as outlined in Sect. 2.3 and described in further detail by Irwin et al. (2010). Calculations of  $S_{c,D_0}$  were not possible for  $D_0 \leq 30 \text{ nm}$  or  $D_0 \geq 200 \text{ nm}$  as the critical supersaturation of the aerosol at these sizes was outside of the supersaturation range measured by the instrumentation.

$GF_{D_0,RH,mean,corr}$  is plotted against both  $S_{c(\kappa,GF_{D_0,RH,mean,corr})}$  (circles) and  $S_{c,D_0}$  (crosses) for the size range  $20 \text{ nm} \leq D_0 \leq 200 \text{ nm}$  and is shown in Fig. 4). The box

## Reconciliation of hygroscopicity measurements during UK-COPS

M. Irwin et al.

Title Page

Abstract

Introduction

Conclusions

References

Tables

Figures

⏪

⏩

◀

▶

Back

Close

Full Screen / Esc

Printer-friendly Version

Interactive Discussion



## Reconciliation of hygroscopicity measurements during UK-COPS

M. Irwin et al.

Title Page

Abstract

Introduction

Conclusions

References

Tables

Figures

⏪

⏩

◀

▶

Back

Close

Full Screen / Esc

Printer-friendly Version

Interactive Discussion



plots in Fig. 4 show the median, 25th and 75th percentiles of the model predicted critical supersaturation,  $S_{c(\kappa, GF_{D_0, RH, mean, corr})}$ , using the range of mean growth factor measured at the size denoted by colour and the whiskers denote the 10th and 90th percentiles of these predictions. The growth factors for ammonium sulphate are also plotted against their respective  $S_{c, D_0}$  for comparison. The coloured circles indicate the predicted  $S_{c(\kappa, GF_{D_0, RH, mean, corr})}$  for a given growth factor (and assumed surface tension,  $\sigma$ ) for guidance. The crosses represent the measured data pairs of mean growth factor  $GF_{D_0, RH, mean, corr}$  and  $S_{c, D_0}$ , with the particle dry size represented by its colour. The error bars show the standard error associated with each data point; propagated from primary data quantities (Irwin et al., 2010). For dry sizes  $D_0=43$  nm, 85 nm there is a clear tendency for the model to over-predict  $S_{c(\kappa, GF_{D_0, RH, mean, corr})}$ , with  $S_{c, D_0}$  falling far outside of the box plots beyond the measurement uncertainty, indicating an inability of the model to predict critical supersaturation at these sizes within instrumental uncertainties. At 121/127 nm, better agreement between model and measurement is seen, but still with a slight bias towards overpredicting the critical supersaturation. At  $D_0$  of 174/169 nm similar agreement between model and measurement is seen, but with the bias reversing and underpredicting critical supersaturation. All data points have been ascribed a transparency according to the degree of multimodality in the growth factor distribution using the difference between mean ( $GF_{D_0, 86\%, mean, corr}$ ) and peak ( $GF_{D_0, 86\%, peak, corr}$ ) growth factor as a qualitative indicator. The solid crosses represent points where these values deviate by less than 5%, intermediate transparency points for between 5 and 10% deviation and the most transparent values for points where the mean and peak growth factors deviate by more than 10%. It can be seen that an almost identical trend is followed irrespective of the multimodal nature of the distribution with the best agreement at the largest sizes. So, even when nominally monomodal ( $GF_{D_0, 86\%, mean, corr}$  within 5% of the  $GF_{D_0, 86\%, peak, corr}$ ), reconciliation of sub- and supersaturated measurements at  $D_0=43$  nm or 85 nm are not achieved within measurement uncertainty.

Hygroscopicity parameters derived from the sub- and supersaturated water uptake measurements,  $\kappa_{S_{c, D_0}}$  and  $\kappa_{GF_{D_0}}$  are plotted in Fig. 5 with their associated errors (as de-

scribed in Sect. 2.6 and Irwin et al., 2010). These data are further tabulated in Tables 2 and 3, where  $\kappa$  values have been sectorised according to the organic:sulphate ratio. The greatest discrepancy is observed at smaller particle sizes, with  $\kappa_{S_c, D_0}$  systematically greater than  $\kappa_{GF, D_0}$  and well outside measurement uncertainty. The  $\kappa$ -values move into closer agreement with increasing size, until at 169 nm diameter, the average  $\kappa_{GF, D_0}$  is slightly greater than the  $\kappa_{S_c, D_0}$ .

No size-dependent systematic difference was found between the HTDMA and CCNc derived  $S_c$  of particles with different organic to sulphate ratios. Figure 6 shows the HTDMA derived and CCNc derived critical supersaturations, coloured according to their organic:sulphate ratio. The left panel of Fig. 6 shows that for the larger sizes of 127 nm and above, the critical supersaturation as predicted from hygroscopicity parameterisation of the HTDMA data is higher during periods of a high organic to sulphate ratio, than when sulphate dominated. However, this is not consistent at all sizes, and when comparing to the critical supersaturations as derived from CCNc data, there is no clear relationship between particle composition and water affinity.

The mean  $\kappa$  for both CCNc and HTDMA data is slightly higher ( $\kappa_{S_c, D_0, avg} = 0.292 \pm 0.128$ ,  $\kappa_{GF, D_0, RH, mean, corr, avg} = 0.181 \pm 0.056$ ) with increased relative sulphate contribution, indicating a slightly more hygroscopic aerosol than when the organic:sulphate ratio is high ( $\kappa_{S_c, D_0, avg} = 0.283 \pm 0.069$ ,  $\kappa_{GF, D_0, RH, mean, corr, avg} = 0.142 \pm 0.036$ ; Tables 2 and 3), as might be expected. Size-resolved AMS data (Fig. S3 in supplementary material) shows a markedly higher organic fraction at sizes greater than 100 nm in both periods of low and high organic fraction, possibly resulting in the lack of difference in water uptake between periods of high and low organic to sulphate ratio shown in Tables 2 and 3.

In numerous cases, the mean growth factor either matches the peak value or is too close for an error bar to be visible but there are cases for which the mean growth factor deviates, typically to lower values, from the peak of the hygroscopic mode due to a background of less hygroscopic particles. Even when screening for bimodality,

## Reconciliation of hygroscopicity measurements during UK-COPS

M. Irwin et al.

Title Page

Abstract

Introduction

Conclusions

References

Tables

Figures

⏪

⏩

◀

▶

Back

Close

Full Screen / Esc

Printer-friendly Version

Interactive Discussion

the  $\kappa$ -Köhler model fails to accurately predict the CCNc derived  $S_c$ , and the decrease in the discrepancy between model and measurement with larger particle size cannot be solely due to the previously discussed increase in hygroscopic bimodality of the aerosol at larger sizes. It can be seen from the lack of difference between points of varying transparency that the bimodality in aerosol mixing state with respect to growth factor cannot be the only reason for the discrepancy in the HTDMA and CCNc derived  $\kappa$ -values.

### 3.6 Potential cloud droplet number concentrations

For each supersaturation, assuming internal mixing with respect to CCN activity, the aerosol will have a corresponding threshold dry diameter above which the aerosol particles activate into cloud droplets. Therefore, assuming no competition between droplets for water vapour, it is possible to estimate the maximum potential cloud droplet number concentration (CDNC) at the given supersaturation by integrating the DMPS size distribution from the largest diameter bin to this threshold diameter.

The threshold diameter for activation were derived from CCNc measurement via three pathways (explained in detail in Irwin et al., 2010):

two threshold diameters for activation can be derived from CCNc critical supersaturation data;  $D_{\text{thres}(\kappa, S_c)}$ , where the hygroscopicity parameter  $\kappa_{S_c, D_0}$  is used to derive  $D_{\text{thres}(\kappa, S_c)}$  by the use of a  $\kappa$  lookup table at 1 nm and  $0.01\kappa$  resolution. The  $\kappa$  value is then inserted into Eq. (3) and for a given  $S_{\text{set}}$  (effectively  $S_c$ ), the threshold diameter for activation can be calculated. Alternatively, the calculation can be performed without the use of a hygroscopicity parameter, in the same fashion as for calculating the threshold diameter for activation from  $D_{50, S}$ ;  $S_{c, D_0} - S_{\text{set}}$  is plotted against  $D_0$  and the intercept defines  $D_{\text{thres}(S_c, D_0)}$ , shown in Fig. S4 in supplementary material. A clear benefit of the latter method is that less calculations are performed, thus not increasing the propagated errors further. However, a significant drawback is that this technique only works for interim supersaturations.

## Reconciliation of hygroscopicity measurements during UK-COPS

M. Irwin et al.

Title Page

Abstract

Introduction

Conclusions

References

Tables

Figures

⏪

⏩

◀

▶

Back

Close

Full Screen / Esc

Printer-friendly Version

Interactive Discussion



The most direct method is to plot  $D_{50,S}-D_0$  vs.  $D_0$ , where the intercept represents the physical threshold diameter for activation of the aerosol,  $D_{\text{thres}(D_{50,S})}$  (in a similar manner to Fig. S4 in supplementary material).

In addition, a threshold diameter for activation can be derived from the HTDMA derived derived hygroscopicity parameter  $\kappa_{(\text{GF}_{D_0})}$ . As there are 7 dry sizes scanned by the HTDMA, each dry size has an associated  $\text{GF}_{D_0, \text{RH, mean, corr}}$  and thus  $\kappa$ . As with previous calculations, the intercept of  $D_{\text{thres}}-D_0$  vs.  $D_0$  defines the HTDMA  $D_{\text{thres}(\kappa, \text{GF})}$ .

The potential CDNC calculation is most sensitive to the threshold diameter for activation around the peak of the aerosol size distribution, and is heavily dependent on the position and breadth of this peak. Out of cloud measurements were typically characterised by a monomodal distribution with a peak around 100 nm and with typical  $40 \text{ nm} \leq D_{\text{thres}} \leq 180 \text{ nm}$ , the difference in potential CDNC is affected greatly by this mode. Figure 7a shows the largest difference in potential CDNC between the hygroscopicity parameter derived HTDMA and CCNc  $D_{\text{thres}}$  analysis occurs at the lowest supersaturation (0.11%). Even though the mean difference in  $D_{\text{thres}}$  is 12% ( $D_{\text{thres}(\text{GF})}=182 \text{ nm}$ ,  $D_{\text{thres}(\kappa, S_c)}=163 \text{ nm}$ ), the difference in potential CDNC is 40%. For all supersaturations, the disagreement between the predictions of CDNC is greater than 30%. In contrast, Fig. 7b shows the smallest difference in potential CDNC between  $D_{\text{thres}(\kappa, \text{GF})}$  and  $D_{\text{thres}(D_{50,S})}$  at the lowest supersaturation. This is due to the increased proximity of  $D_{\text{thres}(\kappa, \text{GF})}=182 \text{ nm}$ ,  $D_{\text{thres}(D_{50,S})}=184 \text{ nm}$ . Excluding the measurement at the lowest supersaturation, the results follow a similar pattern as seen in Fig. 7. It can be seen that the discrepancies are usually outside the attributable errors and cannot be easily reconciled.

## 4 Discussion

Using the  $\kappa$ -Köhler model to predict CCN activity based on sub and supersaturated particle water uptake measurements, the strongest agreement is between the HTDMA and CCNc  $D_{50,S}$  analysis. Agreement is strongest most notably at the lowest super-

### Reconciliation of hygroscopicity measurements during UK-COPS

M. Irwin et al.

Title Page

Abstract

Introduction

Conclusions

References

Tables

Figures

⏪

⏩

◀

▶

Back

Close

Full Screen / Esc

Printer-friendly Version

Interactive Discussion



saturation setting; where activation diameters are typically mid-range of the DMPS size-distribution (improving fitting statistics). Reconciliation between the HTDMA and CCNc using the hygroscopicity parameter  $\kappa$  results in the weakest overall agreement. Figure 5 shows that only for the 127/121 nm and 169/174 nm measurements do values of  $\kappa$  approach the 1:1 line; though the error associated with  $\kappa_{S_c, D_0}$  reduces the confidence in conclusions drawn from this agreement.

However, it must be noted that at both the lowest and highest supersaturations, the number of data points generated from the  $S_c$  analysis is lower than at intermediate supersaturations as fitting is only successful if  $S_{\min} \leq S_c \leq S_{\max}$ , and as such the results are biased towards values where critical supersaturation for a threshold diameter for activation is bounded by  $S_{\text{set}}$ . This is further illustrated by Fig. 6; the predicted critical supersaturations for all sizes, with the exception of 127 nm, have points which fall outside of the  $S_{\text{set}}$  range. This creates an artificial floor and ceiling to the critical supersaturation data derived from the CCNc, and even at 121 nm, some of the derivations lead to uncertainty falling outside of this range. This may explain why at 121/127 nm the  $\kappa$  values derived from each instrument show best agreement (Fig. 5), and also go some way to explain how the size dependence of  $\kappa_{S_c, D_0}$  is reversed to that of the HTDMA (Tables 2 and 3).

The segregation of the data into single mode (mean growth factor  $\leq 5\%$  of the peak bin), and multi-mode (mean growth factor  $\geq 10\%$  of the peak bin) could not explain the disagreement between the two instruments. No clear influence of mixing state was found when comparing the derived hygroscopicity parameters from both instruments (Fig. 5).

This study was performed with the assumption that the growing cloud droplets have a surface tension equal to that of water ( $72.5 \text{ mNm}^{-1}$  at 298 K) at the point of activation. The model represents the measured critical supersaturations at 174/169 nm well, using a surface tension of  $72.5 \text{ mNm}^{-1}$  (Fig. 4). In order to bring the model predictions into agreement with the measured CCN activity for the dry sizes of 121/127 nm and below, surface tensions ranging from  $50 \text{ mNm}^{-1}$  to  $70 \text{ mNm}^{-1}$  must be assumed, with

## Reconciliation of hygroscopicity measurements during UK-COPS

M. Irwin et al.

[Title Page](#)[Abstract](#)[Introduction](#)[Conclusions](#)[References](#)[Tables](#)[Figures](#)[⏪](#)[⏩](#)[◀](#)[▶](#)[Back](#)[Close](#)[Full Screen / Esc](#)[Printer-friendly Version](#)[Interactive Discussion](#)

the smallest sizes requiring the smallest surface tension. It is not clear that any atmospherically reasonable organic compounds at the concentration found at the point of activation can lead to the larger surface tension suppressions. Furthermore, one might assume that a clear relationship between organic:sulphate ratio and critical supersaturation would emerge if the suppression of surface tension greatly influenced the cloud activation behaviour.

Surface tensions of multicomponent mixtures are not readily predictable even in bulk solutions (Topping et al., 2005). Bulk to surface partitioning has been postulated as a potentially important phenomena which can increase the predicted critical saturation ratio required for droplet activation through removal of material used to calculate the Raoult term in the Kohler equation (Eq. 1). Neglecting bulk-to-surface partitioning has been shown to result in an underestimation of  $S_c$  (Sorjamaa et al., 2004, 2006) and that the smaller the particle, the greater the effect of surface to bulk partitioning (Sorjamaa et al., 2004). However, for this study all calculations have neglected the partitioning of material between a bulk and surface layer. An overestimation of  $S_c$  is seen for all sizes below 121/127 nm, above which better agreement is seen between the predicted  $S_c$  and measured  $S_c$ , indicating that if the effects of bulk to surface partitioning were to be included, predicted  $S_c$  would further deviate from measured  $S_c$ .

Segregating the data into periods of high and low sulphate to organic ratio (Fig. S2 in supplementary material and even using size resolved AMS data (Fig. S3 in supplementary material) resulted in no systematic improvement or degradation to the agreement between the predicted and measured data (Fig. 4). Whilst the model leads to better agreement for sizes of 121/127 nm and above (Fig. 4), the reason for the apparent agreement is unclear. The influence of bimodality on the mean growth factor cannot explain the difference between  $\kappa_{(GF_{D_0})}$  and  $\kappa_{S_c, D_0}$ , as strongly monomodal aerosol does not conclusively show this to be the reason behind the apparent discrepancy (Fig. 5). The lack of influence of the organic:sulphate ratio on particle hygroscopicity could suggest a predominantly internally mixed aerosol, or a main growth factor mode encapsulating a spectrum of compositions. An internally mixed aerosol will appear to

## Reconciliation of hygroscopicity measurements during UK-COPS

M. Irwin et al.

Title Page

Abstract

Introduction

Conclusions

References

Tables

Figures



Back

Close

Full Screen / Esc

Printer-friendly Version

Interactive Discussion



be well represented by the mean growth factor, and a spectrum of compositions may appear as one broad mode. This would be lost within the CCNc data as the resolution of the instrument would not pick out these particles of varied composition. In theory, this broadens the ideal step function in activation space of the CCNc, yet with only 5 supersaturations for each  $D_0$ , the fitted sigmoid function is reasonably broad initially and a spread of compositions would not be resolved in this manner. It is also unlikely that a change in surface tension can explain the disagreement, as surface tensions as low as  $50 \text{ mNm}^{-1}$  are not expected.

## 5 Conclusions

Measurements of aerosol hygroscopic growth, CCN activity and composition were made simultaneously and have been used to probe the applicability of a single parameter representation of aerosol water uptake. It was found that changes in the organic:sulphate ratio did result in variations in aerosol hygroscopicity at 86% RH but no systematic variation in the CCN activity of the aerosol was found. Periods of measurement conducted “in cloud” were typically characterised by low number concentrations, a lower organic:sulphate ratio and a higher hygroscopic mean growth factor. “No cloud” periods were characterised by higher aerosol concentrations across the size range, an increased organic:sulphate ratio and a lower hygroscopic mean growth factor. Whilst variations in the CCN fraction are evident they could not be directly linked to changes in composition, in part due to the variations in mixing state of the aerosol during different periods.

Corrected mean growth factors at 86% RH as measured by the HTDMA at multiple  $D_0$  were used to derive the hygroscopicity parameter  $\kappa$ . The  $\kappa$ -Köhler model was used to predict both critical supersaturations and threshold diameters for activation from the data. Critical supersaturation was derived as a function of dry size by the CCNc and was compared to the HTDMA  $\kappa$ -model derived critical supersaturation with varying results. When comparing  $\kappa$  derived products from each instrument, the dis-

## Reconciliation of hygroscopicity measurements during UK-COPS

M. Irwin et al.

Title Page

Abstract

Introduction

Conclusions

References

Tables

Figures



Back

Close

Full Screen / Esc

Printer-friendly Version

Interactive Discussion



crepancy appears largest for the most atmospherically relevant supersaturations with the most significant difference being a 56% difference in CDNC at the lowest supersaturation (0.11%), with higher supersaturations (0.17–0.80%) resulting in less difference between prediction and measurement (53%–18%), shown in Fig. 7.

CCNc data was also analysed without the use of the hygroscopicity parameter  $\kappa$ , but in terms of the threshold dry diameter for activation,  $D_{50,S}$ . The  $D_{50,S}$  analysis had the best agreement with the HTDMA derived CDNC at the lowest supersaturation with an 8% difference, but for the rest of the supersaturation range there was a decreasing over-estimate with supersaturation (26%–18%). Data which falls closest to the centre of the ranges of dry size selection and supersaturation are less susceptible to bias from instrument limitations and as such generated more data points with reduced standard error than those made at the limits of the CCN instrument.

Further to this, the physical activation diameter of the aerosol was derived directly from  $S_{c,D_0}$  by plotting the intercept of  $S_{c,D_0} - S_{\text{set}}$  vs.  $S_{\text{set}}$ . Whilst this method could only derive  $D_{\text{thres}}$  for the latter-half interim supersaturations of 0.17%, 0.32% and 0.50%, there is only between 20–27% over estimation when compared to the HTDMA derived CDNC.

Measurement uncertainty has been propagated through to derived products for each calculation presented in the paper. The inclusion and propagation of these errors has allowed an assessment on the reconciliation ability of the instruments to take place. The disagreement between the derived products is far outside instrument instrument uncertainty and as such, attempts have been made to uncover the reason for this disagreement. Mixing state has not resulted in clear, systematic differences between the products and neither has the segregation of the data into periods dominated by sulphate or organic composition. What is clear, is that the instrumentation shows the best agreement when the derived products are able to be measured wholly from either instrument, i.e. the best agreement between CCNc and HTDMA occurs when the range of supersaturations measured by the CCNc are such that they allow for the entire  $S_c$  range of a particular size. Should particles of a given diameter have critical super-

## Reconciliation of hygroscopicity measurements during UK-COPS

M. Irwin et al.

Title Page

Abstract

Introduction

Conclusions

References

Tables

Figures

⏪

⏩

◀

▶

Back

Close

Full Screen / Esc

Printer-friendly Version

Interactive Discussion



saturations that cannot be derived by the CCNc but can be predicted by the HTDMA, results will surely diverge.

Whilst the  $\kappa$ -Köhler model has been shown to work for a variety of different compositions (Petters and Kreidenweis, 2007, 2008) and previous  $\kappa$ -Köhler closure attempts ambient CCNc and HTDMA measurements have shown agreement to within approximately 20% (Carrico et al., 2008), it appears not to be the case for the ambient measurements in this study unless surface properties are changed, probably unrealistically. In addition, the inclusion of bulk to surface partitioning would lead to an increased discrepancy between the derived values of  $S_c$ , illustrating a possible need for caution in the generalised application of this single parameter approximation in ambient atmospheric studies until reasons for the highlighted discrepancies are understood. Obviously the use of  $\kappa$  values differing by as much as those derived from our HTDMA and CCN measurements in this study would result in differences in predicted aerosol indirect effects corresponding to the significant difference in potential CDNC as reported.

**Supplementary material related to this article is available online at:**  
**<http://www.atmos-chem-phys-discuss.net/10/17073/2010/acpd-10-17073-2010-supplement.pdf>.**

*Acknowledgements.* The UK Convective and Orographically-induced Precipitation Study (UK-COPS) was funded by the National Environmental Research Council (NERC) (NE/E016200/1) and NERC Ph.D Studentship of Martin Irwin (NER/S/A/2006/14036). The authors wish to thank Michael Flynn and Keith Bower for their assistance in the field.

## References

Abdul-Razzak, H. and Ghan, S. J.: Parameterization of the influence of organic surfactants on aerosol activation, *J. Geophys. Res.-Atmos.*, 109, D03205, doi:10.1029/2003JD004043, 2004. 17076

## Reconciliation of hygroscopicity measurements during UK-COPS

M. Irwin et al.

Title Page

Abstract

Introduction

Conclusions

References

Tables

Figures



Back

Close

Full Screen / Esc

Printer-friendly Version

Interactive Discussion



## Reconciliation of hygroscopicity measurements during UK-COPS

M. Irwin et al.

Title Page

Abstract

Introduction

Conclusions

References

Tables

Figures

⏪

⏩

◀

▶

Back

Close

Full Screen / Esc

Printer-friendly Version

Interactive Discussion



- Albrecht, B.: Aerosols, cloud microphysics, and fractional cloudiness, *Science*, 245(4923), 1227, doi:10.1126/science.245.4923.1227, 1989. 17075
- Andreae, M. and Rosenfeld, D.: Aerosol-cloud-precipitation interactions. Part 1. The nature and sources of cloud-active aerosols, *Earth Sci. Rev.*, 89(1–2), 13–41, 2008. 17075, 17077
- 5 Broekhuizen, K., Chang, R. Y.-W., Leaitch, W. R., Li, S.-M., and Abbatt, J. P. D.: Closure between measured and modeled cloud condensation nuclei (CCN) using size-resolved aerosol compositions in downtown Toronto, *Atmos. Chem. Phys.*, 6, 2513–2524, doi:10.5194/acp-6-2513-2006, 2006. 17076
- Carrico, C., Petters, M., and Kreidenweis, S.: Aerosol hygroscopicity and cloud droplet activation of extracts of filters from biomass burning experiments, *J. Geophys. Res.-Atmos.*, 113, D08206, doi:10.1029/2007JD009274, 2008. 17096
- 10 Cubison, M. J., Coe, H., and Gysel, M.: A modified hygroscopic tandem DMA and a data retrieval method based on optimal estimation, *J. Aerosol Sci.*, 36, 846–865, 2005. 17077, 17078
- 15 Decarlo, P., Slowik, J., Worsnop, D., Davidovits, P., and Jimenez, J.: Particle morphology and density characterization by combined mobility and aerodynamic diameter measurements. Part 1: theory, *Aerosol Sci. Tech.*, 38, 1185–1205, doi:10.1080/027868290903907, 2004. 17081, 17087
- DeCarlo, P., Kimmel, J., Trimborn, A., Northway, M., Jayne, J., Aiken, A., Gonin, M., Fuhrer, K., Horvath, T., Docherty, K., Worsnop, D., and Jimenez, J. L.: Field-deployable, high-resolution, time-of-flight aerosol mass spectrometer, *Anal. Chem.*, 78, 8281–8289, 2006. 17081
- 20 Fachini, M. C., Decesari, S., Mircea, M., Fuzzi, S., and Loglio, G.: Surface tension of atmospheric wet aerosol and cloud/fog droplets in relation to their organic carbon content and chemical composition, *Atmos. Environ.*, 33, 4853–4857, 2000. 17076
- 25 Forster, P., Ramaswamy, V., Artaxo, P., Berntsen, T., Betts, R., Fahey, D., Haywood, J., Lean, J., Lowe, D., Myhre, G., Nganga, J., Prinn, R., Raga, G., Schulz, M., and Dorland, R. V.: Changes in Atmospheric Constituents and in Radiative Forcing, in: *Climate Change 2007: The Physical Science Basis*, Contribution of Working Group I to the Fourth Assessment Report of the Intergovernmental Panel on Climate Change, 2007. 17075
- 30 Good, N., Coe, H., and McFiggans, G.: Instrumentational operation and analytical methodology for the reconciliation of aerosol water uptake under sub- and supersaturated conditions, *Atmos. Meas. Tech. Discuss.*, 3, 359–403, doi:10.5194/amtd-3-359-2010, 2010. 17078, 17081
- Gunthe, S. S., King, S. M., Rose, D., Chen, Q., Roldin, P., Farmer, D. K., Jimenez, J. L.,

**Reconciliation of  
hygroscopicity  
measurements  
during UK-COPS**

M. Irwin et al.

Title Page

Abstract

Introduction

Conclusions

References

Tables

Figures

⏪

⏩

◀

▶

Back

Close

Full Screen / Esc

Printer-friendly Version

Interactive Discussion



Artaxo, P., Andreae, M. O., Martin, S. T., and Pöschl, U.: Cloud condensation nuclei in pristine tropical rainforest air of Amazonia: size-resolved measurements and modeling of atmospheric aerosol composition and CCN activity, *Atmos. Chem. Phys.*, 9, 7551–7575, doi:10.5194/acp-9-7551-2009, 2009. 17077

5 Gysel, M., Crosier, J., Topping, D. O., Whitehead, J. D., Bower, K. N., Cubison, M. J., Williams, P. I., Flynn, M. J., McFiggans, G. B., and Coe, H.: Closure study between chemical composition and hygroscopic growth of aerosol particles during TORCH2, *Atmos. Chem. Phys.*, 7, 6131–6144, doi:10.5194/acp-7-6131-2007, 2007. 17077, 17078

Gysel, M., McFiggans, G., and Coe, H.: Inversion of tandem differential mobility analyser (TDMA) measurements, *J. Aerosol Sci.*, 40, 134–151, 2009. 17078, 17079

10 Hallquist, M., Wenger, J. C., Baltensperger, U., Rudich, Y., Simpson, D., Claeys, M., Dommen, J., Donahue, N. M., George, C., Goldstein, A. H., Hamilton, J. F., Herrmann, H., Hoffmann, T., Iinuma, Y., Jang, M., Jenkin, M. E., Jimenez, J. L., Kiendler-Scharr, A., Maenhaut, W., McFiggans, G., Mentel, Th. F., Monod, A., Prévôt, A. S. H., Seinfeld, J. H., Surratt, J. D., Szmigielski, R., and Wildt, J.: The formation, properties and impact of secondary organic aerosol: current and emerging issues, *Atmos. Chem. Phys.*, 9, 5155–5236, doi:10.5194/acp-9-5155-2009, 2009. 17076

Haywood, J. and Boucher, O.: Estimates of the direct and indirect radiative forcing due to tropospheric aerosols: a review, *Rev. Geophys.*, 38, 513–543, 2000. 17074

20 Irwin, M., Allan, J. D., and McFiggans, G.: Error analysis in the reconciliation of measured aerosol water uptake in sub- and supersaturated regimes, *Atmos. Meas. Tech. Discuss.*, in review, 2010. 17079, 17080, 17081, 17087, 17088, 17089, 17090, 17111

Kanakidou, M., Seinfeld, J. H., Pandis, S. N., Barnes, I., Dentener, F. J., Facchini, M. C., Van Dingenen, R., Ervens, B., Nenes, A., Nielsen, C. J., Swietlicki, E., Putaud, J. P., Balkanski, Y., Fuzzi, S., Horth, J., Moortgat, G. K., Winterhalter, R., Myhre, C. E. L., Tsigaridis, K., Vignati, E., Stephanou, E. G., and Wilson, J.: Organic aerosol and global climate modelling: a review, *Atmos. Chem. Phys.*, 5, 1053–1123, doi:10.5194/acp-5-1053-2005, 2005. 17076

Köhler, H.: The nucleus in and the growth of hygroscopic droplets, *T. Faraday Soc.*, 32, 1152–1161, doi:10.1039/TF9363201152, 1936. 17075

30 Lance, S., Medina, J., Smith, J., and Nenes, A.: Mapping the operation of the DMT continuous flow CCN counter, *Aerosol Sci. Tech.*, 40(4), 242–254, doi:10.1080/02786820500543290, 2006. 17079

Lohmann, U. and Feichter, J.: Global indirect aerosol effects: a review, *Atmos. Chem. Phys.*, 5,

**Reconciliation of  
hygroscopicity  
measurements  
during UK-COPS**

M. Irwin et al.

[Title Page](#)[Abstract](#)[Introduction](#)[Conclusions](#)[References](#)[Tables](#)[Figures](#)[⏪](#)[⏩](#)[◀](#)[▶](#)[Back](#)[Close](#)[Full Screen / Esc](#)[Printer-friendly Version](#)[Interactive Discussion](#)

715–737, doi:10.5194/acp-5-715-2005, 2005. 17075

Matthew, B. M., Middlebrook, A., and Onasch, T.: Collection efficiencies in an aerodyne aerosol mass spectrometer as a function of particle phase for laboratory generated aerosols, *Aerosol Sci. Tech.*, 42, 884–898, doi:10.1080/02786820802356797, 2008. 17081

5 McCormick, R. and Ludwig, J.: Climate modification by atmospheric aerosols, *Science*, 156(3780), 1358–1359, 1967. 17074

McFiggans, G., Alfarra, M., Allan, J., Bower, K., and Coe, H.: Simplification of the representation of the organic component of atmospheric particulates, *Faraday Discuss.*, 130, 341–362, 2005. 17076

10 McFiggans, G., Artaxo, P., Baltensperger, U., Coe, H., Facchini, M. C., Feingold, G., Fuzzi, S., Gysel, M., Laaksonen, A., Lohmann, U., Mentel, T. F., Murphy, D. M., O'Dowd, C. D., Snider, J. R., and Weingartner, E.: The effect of physical and chemical aerosol properties on warm cloud droplet activation, *Atmos. Chem. Phys.*, 6, 2593–2649, doi:10.5194/acp-6-2593-2006, 2006. 17075, 17076

15 Medina, J., Nenes, A., Sotiropoulou, R., and Cottrell, L.: Cloud condensation nuclei closure during the international consortium for atmospheric research on transport and transformation 2004 campaign: effects of size-resolved composition, *J. Geophys. Res.*, 112, D10S31, doi:10.1029/2006JD007588, 2007. 17076

Petters, M. D. and Kreidenweis, S. M.: A single parameter representation of hygroscopic growth and cloud condensation nucleus activity, *Atmos. Chem. Phys.*, 7, 1961–1971, doi:10.5194/acp-7-1961-2007, 2007. 17076, 17096

Petters, M. D. and Kreidenweis, S. M.: A single parameter representation of hygroscopic growth and cloud condensation nucleus activity – Part 2: Including solubility, *Atmos. Chem. Phys.*, 8, 6273–6279, doi:10.5194/acp-8-6273-2008, 2008. 17096

25 Petters, M., Prenni, A. J., Kreidenweis, S. M., and DeMott, P. J.: On measuring the critical diameter of cloud condensation nuclei using mobility selected aerosol, *Aerosol Sci. Tech.*, 41, 907–913, 2007. 17082

Pruppacher, H. and Klett, J.: *Microphysics of Clouds and Precipitation*, 18, Kluwer Acad., Norwell, Mass., 1997. 17075

30 Roberts, G. C. and Nenes, A.: A continuous-flow streamwise thermal-gradient CCN chamber for atmospheric measurements, *Aerosol Sci. Tech.*, 39, 206–221, 2005. 17079

Rogers, R. R. and Yau, M. K.: *A Short Course in Cloud Physics*, Rogers, R. R., Elmsford (NY, USA), Pergamon Press, 227 pp., 1989. 17075

**Reconciliation of  
hygroscopicity  
measurements  
during UK-COPS**

M. Irwin et al.

Title Page

Abstract

Introduction

Conclusions

References

Tables

Figures

◀

▶

◀

▶

Back

Close

Full Screen / Esc

Printer-friendly Version

Interactive Discussion



Rose, D., Gunthe, S. S., Mikhailov, E., Frank, G. P., Dusek, U., Andreae, M. O., and Pöschl, U.: Calibration and measurement uncertainties of a continuous-flow cloud condensation nuclei counter (DMT-CCNC): CCN activation of ammonium sulfate and sodium chloride aerosol particles in theory and experiment, *Atmos. Chem. Phys.*, 8, 1153–1179, doi:10.5194/acp-8-1153-2008, 2008. 17079

Seinfeld, J. and Pandis, S.: *Atmospheric Chemistry and Physics: From Air Pollution to Climate Change*, Wiley, New York, 1326 pp., 1998. 17075

Sjogren, S., Gysel, M., Weingartner, E., Alfarra, M. R., Duplissy, J., Cozic, J., Crosier, J., Coe, H., and Baltensperger, U.: Hygroscopicity of the submicrometer aerosol at the high-alpine site Jungfraujoch, 3580 m a.s.l., Switzerland, *Atmos. Chem. Phys.*, 8, 5715–5729, doi:10.5194/acp-8-5715-2008, 2008. 17087

Sorjamaa, R., Peräniemi, A., Raatikainen, T., and Laaksonen, A.: Cloud formation of particles containing humic-like substances, *Geophys. Res. Lett.*, 33, L10816, doi:10.1029/2006GL026107, 2006. 17076, 17093

Sorjamaa, R., Svenningsson, B., Raatikainen, T., Henning, S., Bilde, M., and Laaksonen, A.: The role of surfactants in Köhler theory reconsidered, *Atmos. Chem. Phys.*, 4, 2107–2117, doi:10.5194/acp-4-2107-2004, 2004. 17076, 17093

Topping, D. O., McFiggans, G. B., Kiss, G., Varga, Z., Facchini, M. C., Decesari, S., and Mircea, M.: Surface tensions of multi-component mixed inorganic/organic aqueous systems of atmospheric significance: measurements, model predictions and importance for cloud activation predictions, *Atmos. Chem. Phys.*, 7, 2371–2398, doi:10.5194/acp-7-2371-2007, 2007. 17076

Topping, D. O., McFiggans, G. B., and Coe, H.: A curved multi-component aerosol hygroscopicity model framework: Part 1 – Inorganic compounds, *Atmos. Chem. Phys.*, 5, 1205–1222, doi:10.5194/acp-5-1205-2005, 2005. 17078, 17080, 17093

Twomey, S.: Influence of pollution on shortwave albedo of clouds, *J. Atmos. Sci.*, 34, 1149–1152, 1977. 17075

Weingartner, E., Laaksonen, A., and Raatikainen, T.: Cloud forming potential of secondary organic aerosol under near atmospheric conditions, *Geophys. Res. Lett.*, 35, L03818, doi:10.1029/2007GL031075, 2008. 17076

Wex, H., Stratmann, F., Topping, D., and McFiggans, G.: The Kelvin versus the Raoult Term in the Köhler Equation, *J. Atmos. Sci.*, 65, 4004–4016, 2008. 17075, 17076

Wiedensohler, A.: An approximation of the bipolar charge distribution for particles in the sub-

## Reconciliation of hygroscopicity measurements during UK-COPS

M. Irwin et al.

Title Page

Abstract

Introduction

Conclusions

References

Tables

Figures

⏪

⏩

◀

▶

Back

Close

Full Screen / Esc

Printer-friendly Version

Interactive Discussion



micron size range, *J. Aerosol Sci.*, 19, 387–389, 1987. 17081

Williams, P. I., McFiggans, G., and Gallagher, M. W.: Latitudinal aerosol size distribution variation in the Eastern Atlantic Ocean measured aboard the FS-Polarstern, *Atmos. Chem. Phys.*, 7, 2563–2573, doi:10.5194/acp-7-2563-2007, 2007. 17081

- 5 Wulfmeyer, V., Behrendt, A., Bauer, H., Kottmeier, C., Corsmeier, U., Blyth, A., Craig, G., Schumann, U., Hagen, M., Crewell, S., Girolamo, P. D., Flamant, C., Miller, M., Montani, A., Mobbs, S., Richard, E., Rotach, M., Arpagaus, M., Russchenberg, H., Schlüssel, P., König, M., Gärtner, V., Steinacker, R., Dorninger, M., Turner, D., Weckwerth, T., Hense, A., and Simmer, C.: A research and development project of the world weather research program for improving quantitative precipitation forecasting in low-mountain regions, *B. Am. Meteorol. Soc.*, 89, 1477–1486, 2008. 17077
- 10

## Reconciliation of hygroscopicity measurements during UK-COPS

M. Irwin et al.

**Table 1.** Approximations for “cloud periods” and “no cloud” periods as defined by RH and GRIMM measurements.

CP1	NC1	CP2	NC2	CP3	NC3
25–29 June	29 June–2 July	2–6 July	6–8 July	8–13 July	13–17 July
CP4	NC4	CP5	NC5		
17–22 July	22–23 July	23–25 July	25–27 July		

Title Page

Abstract

Introduction

Conclusions

References

Tables

Figures

⏪

⏩

◀

▶

Back

Close

Full Screen / Esc

Printer-friendly Version

Interactive Discussion

## Reconciliation of hygroscopicity measurements during UK-COPS

M. Irwin et al.

**Table 2.**  $\kappa$  values for both HTDMA and CCN data, split by an organic:sulphate ratio of  $\leq 4:1$ .  $D_0$  is particle dry diameter and  $\sigma$  is the standard deviation.

$D_0$	$\kappa_{S_c, D_0}$	$\sigma$	$\kappa_{(GF_{D_0})}$	$\sigma$
26 nm			0.137	0.046
43 nm	0.464	0.099	0.129	0.045
85 nm	0.269	0.100	0.147	0.052
121/127 nm	0.211	0.096	0.187	0.057
174/169 nm	0.133	0.051	0.213	0.052
211 nm			0.231	0.055

Title Page

Abstract

Introduction

Conclusions

References

Tables

Figures

◀

▶

◀

▶

Back

Close

Full Screen / Esc

Printer-friendly Version

Interactive Discussion



## Reconciliation of hygroscopicity measurements during UK-COPS

M. Irwin et al.

**Table 3.**  $\kappa$  values for both HTDMA and CCN data, split by an organic:sulphate ratio of  $\geq 4:1$ .  $D_0$  is particle dry diameter and  $\sigma$  is the standard deviation.

$D_0$	$\kappa_{S_c,D_0}$	$\sigma$	$\kappa_{(GF_{D_0})}$	$\sigma$
26 nm			0.139	0.036
43 nm	0.430	0.104	0.084	0.042
85 nm	0.203	0.118	0.090	0.057
121/127 nm	0.131	0.112	0.128	0.072
174/169 nm	0.102	0.062	0.155	0.055
211 nm			0.165	0.069

[Title Page](#)
[Abstract](#)
[Introduction](#)
[Conclusions](#)
[References](#)
[Tables](#)
[Figures](#)
[Back](#)
[Close](#)
[Full Screen / Esc](#)
[Printer-friendly Version](#)
[Interactive Discussion](#)


## Reconciliation of hygroscopicity measurements during UK-COPS

M. Irwin et al.

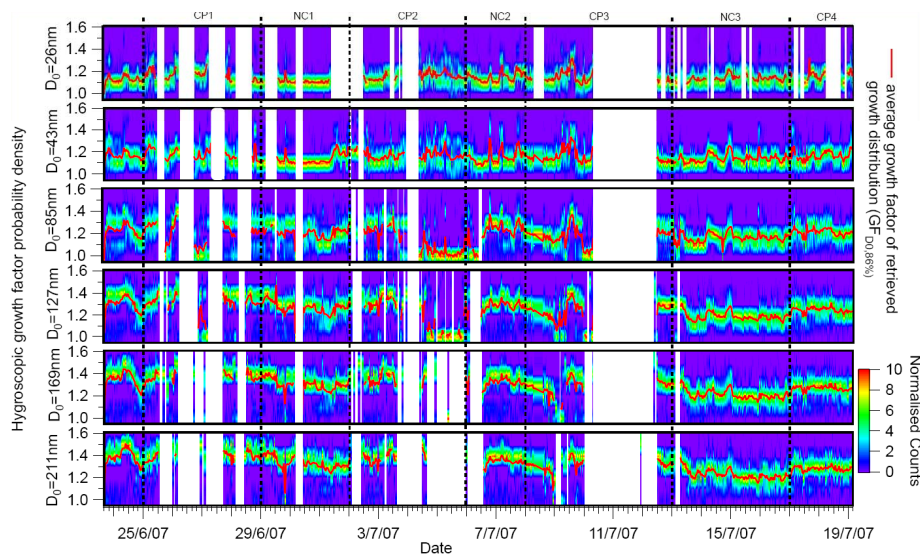


**Fig. 1.** Measured HTDMA hygroscopic growth factor probability density as a function of time. The HTDMA growth factor is typically well represented by the mean growth factor,  $GF_{D_0,86\%}$ . However, there is an increasing prominence of bimodality seen with an increase of size.

Title Page

Abstract

Introduction

Conclusions

References

Tables

Figures



Back

Close

Full Screen / Esc

Printer-friendly Version

Interactive Discussion

## Reconciliation of hygroscopicity measurements during UK-COPS

M. Irwin et al.

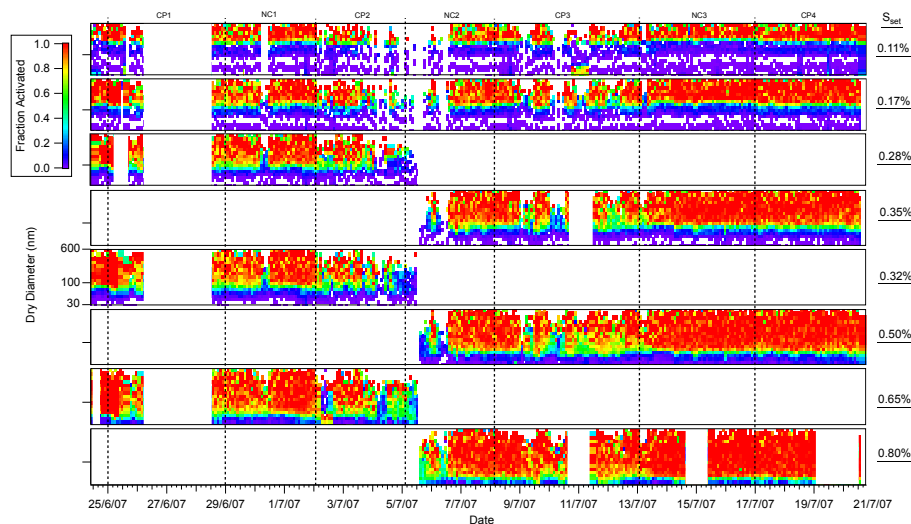


**Fig. 2.** Fraction of CCN activated ( $dF_A/d\log D_p$ ) against time, for each supersaturation setting. The fraction of aerosol activated typically increases with dry size and supersaturation. The decision was made during CP2 to increase the upper limit of the supersaturation setting ( $S_{set}$ ) from 0.65% to 0.80%, in an attempt to activate more of the aerosol below 100 nm.

Title Page

Abstract

Introduction

Conclusions

References

Tables

Figures

⏪

⏩

◀

▶

Back

Close

Full Screen / Esc

Printer-friendly Version

Interactive Discussion

Reconciliation of  
hygroscopicity  
measurements  
during UK-COPS

M. Irwin et al.

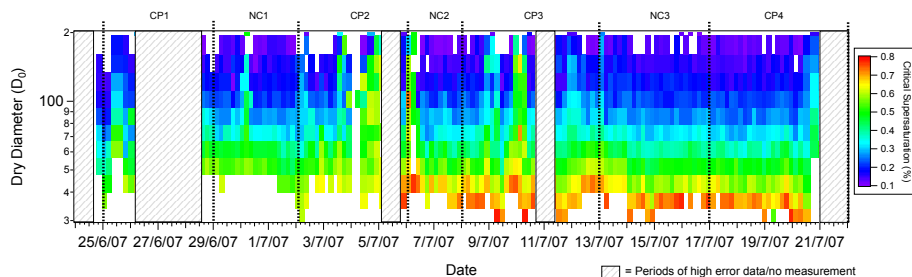


**Fig. 3.** Time series of  $S_c$  vs.  $D_0$  for the duration of the experiment. Larger particles typically require less supersaturation to activate and thus have a lower  $S_c$ . Some variation in  $S_c$  is apparent, but does not correspond strongly to the change in organic:sulphate ratio.

Title Page

Abstract

Introduction

Conclusions

References

Tables

Figures

◀

▶

◀

▶

Back

Close

Full Screen / Esc

Printer-friendly Version

Interactive Discussion

## Reconciliation of hygroscopicity measurements during UK-COPS

M. Irwin et al.

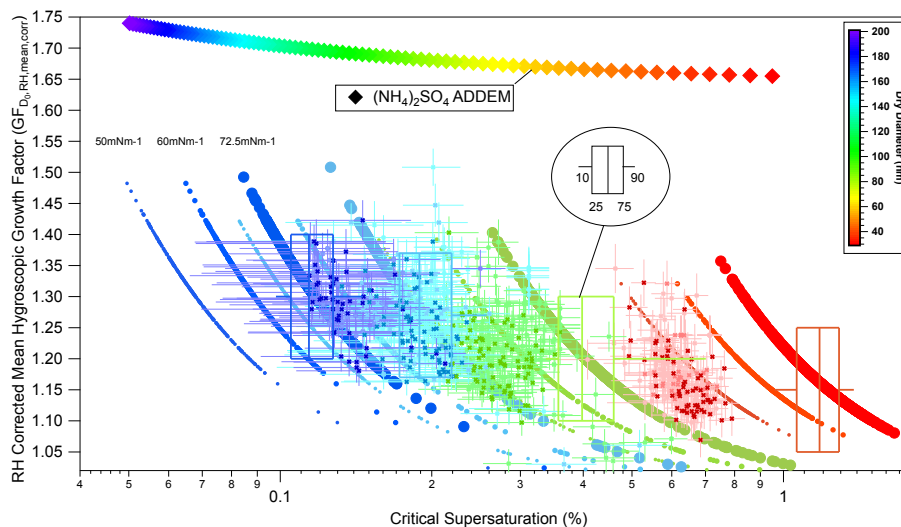


**Fig. 4.**  $GF_{D_0, RH, mean, corr}$  plotted against derived critical supersaturation for  $43 \text{ nm} \leq D_0 \leq 169 \text{ nm}$ . The crosses represent measured data and the circles of increasing diameter represent predictions from the model with three surface tensions;  $50 \text{ mNm}^{-1}$ ,  $60 \text{ mNm}^{-1}$  and  $72.5 \text{ mNm}^{-1}$ , respectively. Error bars are shown in both axis representing the uncertainty in the measured growth factor, and derived  $S_{c, D_0}$ .

[Title Page](#)
[Abstract](#)
[Introduction](#)
[Conclusions](#)
[References](#)
[Tables](#)
[Figures](#)
[⏪](#)
[⏩](#)
[◀](#)
[▶](#)
[Back](#)
[Close](#)
[Full Screen / Esc](#)
[Printer-friendly Version](#)
[Interactive Discussion](#)


## Reconciliation of hygroscopicity measurements during UK-COPS

M. Irwin et al.

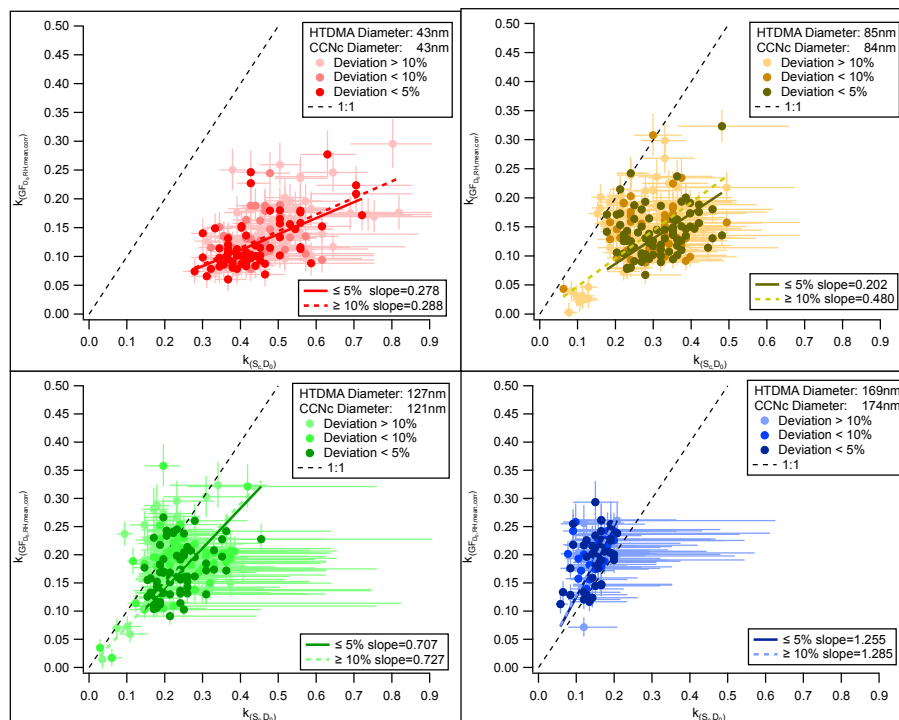


**Fig. 5.**  $K_{(GF_{D_{0,RH,mean,corr}})}$  plotted against  $K_{S_{c,D_0}}$  for the CCN dry diameters closest to those of the measured by the HTDMA. The data is colour weighted according to the proximity of the peak of the growth factor relative to that of the mean growth factor, with the most solid colours representing a deviation below 5%.

Title Page

Abstract

Introduction

Conclusions

References

Tables

Figures

◀

▶

◀

▶

Back

Close

Full Screen / Esc

Printer-friendly Version

Interactive Discussion

## Reconciliation of hygroscopicity measurements during UK-COPS

M. Irwin et al.

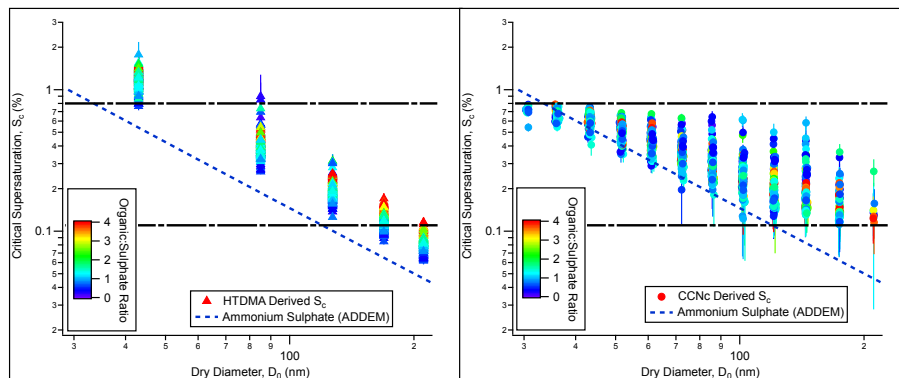


**Fig. 6.** Left panel: a graph showing  $S_{c,GF}$  vs.  $D_0$ , coloured according to organic:sulphate ratio. Right panel: a graph showing  $S_{c,D_0}$  vs.  $D_0$ , coloured according to organic:sulphate ratio. The black dashed line represents the upper and lower values of the supersaturation setting of the CCNc.

Title Page

Abstract

Introduction

Conclusions

References

Tables

Figures

◀

▶

◀

▶

Back

Close

Full Screen / Esc

Printer-friendly Version

Interactive Discussion

Reconciliation of  
hygroscopicity  
measurements  
during UK-COPS

M. Irwin et al.

Title Page

Abstract

Introduction

Conclusions

References

Tables

Figures

◀

▶

◀

▶

Back

Close

Full Screen / Esc

Printer-friendly Version

Interactive Discussion

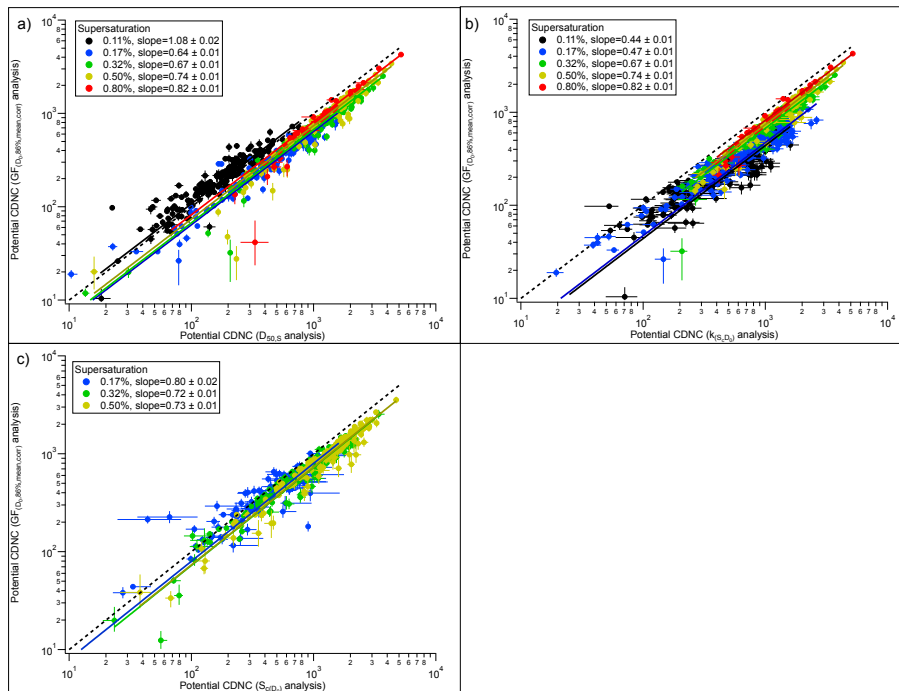


**Fig. 7.** Potential Cloud Droplet Number Concentration (CDNC) as predicted from HTDMA derived  $\kappa$ -Köhler analysis plotted against **(a)** potential CDNC derived from  $D_{50,S}$  analysis, **(b)** potential CDNC derived from  $\kappa_{S_c, D_0}$  analysis, **(c)** potential CDNC derived from  $S_{c, D_0}$  analysis. Where possible, the calculations were performed for the five supersaturation settings. The error bars are the upper and lower bounds in CDNC given as a result of the propagation of errors through the analysis procedure (Irwin et al., 2010). The best fit lines have been plotted using orthogonal distance regression and are weighted according to error.